Organic & Biomolecular Chemistry

www.rsc.org/obc

Volume 8 | Number 13 | 28 June 2010 | Pages 2873–3084

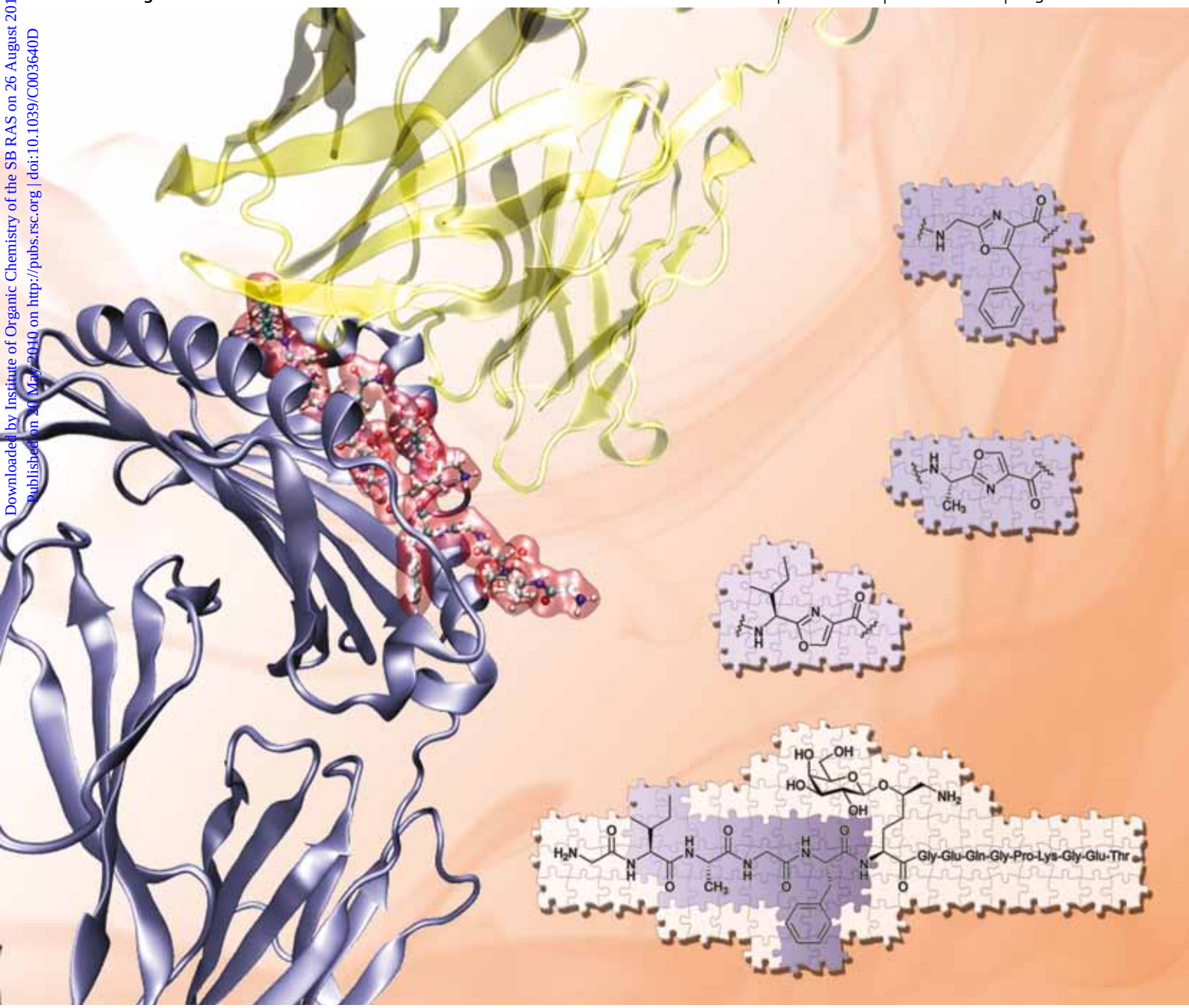

ISSN 1477-0520

RSC Publishing

FULL PAPER
Ida E. Andersson *et al.*
Oxazole-modified glycopeptides that target arthritis-associated class II MHC A^q and DR4 proteins

PERSPECTIVE
Muhammad Moniruzzaman *et al.*
Activation and stabilization of enzymes in ionic liquids

1477-0520(2010)8:13;1-0

Oxazole-modified glycopeptides that target arthritis-associated class II MHC A^q and DR4 proteins†

Ida E. Andersson,[a] Tsvetelina Batsalova,[b] Balik Dzhambazov,[b] Lotta Edvinsson,[a] Rikard Holmdahl,[b] Jan Kihlberg*[a,c] and Anna Linusson*[a]

Received 26th February 2010, Accepted 14th April 2010
First published as an Advance Article on the web 20th May 2010
DOI: 10.1039/c003640d

The glycopeptide CII259-273, a fragment from type II collagen (CII), can induce tolerance in mice susceptible to collagen-induced arthritis (CIA), which is a validated disease model for rheumatoid arthritis (RA). Here, we describe the design and synthesis of a small series of modified CII259-273 glycopeptides with oxazole heterocycles replacing three potentially labile peptide bonds. These glycopeptidomimetics were evaluated for binding to murine CIA-associated A^q and human RA-associated DR4 class II major histocompatibility complex (MHC) proteins. The oxazole modifications drastically reduced or completely abolished binding to A^q. Two of the glycopeptidomimetics were, however, well tolerated in binding to DR4 and they also induced strong responses by one or two DR4-restricted T-cell hybridomas. This work contributes to the development of an altered glycopeptide for inducing immunological tolerance in CIA, with the long-term goal of developing a therapeutic vaccine for treatment of RA.

Introduction

The disease pathology of rheumatoid arthritis (RA), an autoimmune disease that causes chronic inflammation of peripheral cartilaginous joints, can be studied using the mouse model collagen-induced arthritis (CIA).[1] A common feature of human RA and murine CIA is the association with certain antigen-presenting class II major histocompatibility complex (MHC) proteins, *e.g.* DR1 and DR4 in RA,[2–4] and A^q in CIA.[5,6] Class II MHC proteins bind and present peptide antigens to circulating $CD4^+$ T cells, which is a key step in the development of immune and autoimmune responses. T-cell hybridomas obtained from mice with CIA are activated by the CII259-273 glycopeptide, a fragment from type II collagen (CII), when presented by A^q.[7,8] It has been shown in a vaccination study that the CII259-273 glycopeptide can protect mice from developing CIA.[9] More recently, pulmonary vaccination with solubilized A^q protein in complex with CII259-273 was shown to give effective protection against disease development.[10] Arthritis severity was also reduced in mice with an established chronic relapsing disease. If translation of these results to patients suffering from RA would be possible, it would provide completely new approaches to treat and ultimately cure RA. However, a drawback of using glycopeptides as therapeutics is their limited metabolic stability. Introduction of non-peptidic motifs in the CII259-273 glycopeptide to stabilize its structure towards degradation could improve the half-life and thereby its effectiveness as a therapeutic vaccine.

In our ongoing studies to probe A^q binding and T-cell recognition of CII259-273, we have previously used structure-based design to modify parts of the peptide backbone by amide bond replacement with different isosteres. In an initial study, the Ala^{261}-Gly^{262} amide bond was replaced with ketomethylene, (*E*)-alkene, and aminomethylene isosteres.[11] A second study, currently in progress, explores the effects of introducing (*E*)-alkene and ethylene isosteres at the Ile^{260}-Ala^{261}, Ala^{261}-Gly^{262}, and Gly^{262}-Phe^{263} positions.[12] The design of the modified glycopeptides has been guided by a comparative model of the A^q protein[11] (Fig. 1). Experimentally determined binding features support the proposed binding pose of the glycopeptide ligand in the A^q binding site. That is, the side chains of Ile^{260} and Phe^{263} anchor the glycopeptide in the P1 and P4 pockets of A^q while the β-D-galactosyl residue attached to the hydroxylysine side chain ($GalHyl^{264}$) extends out of the binding site to interact with a T-cell receptor approaching from above.[7,8,13–15] T-cell hybridomas specific for CII259-273 with the $GalHyl^{264}$ moiety have also been generated using transgenic mice expressing human DR4 and human CD4 co-receptor,[16] suggesting an important role for this residue in RA as well as CIA. However, compared to the A^q system, the DR4 binding epitope is shifted three amino acids towards the C terminus of CII.[17] Hence, the side chain of Phe^{263} occupies the prominent P1 pocket while the side chain of Glu^{266} is positioned in the shallow P4 pocket in the DR4 binding site.

In this study, we introduce oxazole heterocycles in the CII259-273 backbone as structurally more diverse bioisosteres in comparison to the amide bond isosteres studied previously by us.[11,12] Oxazoles have been described as conformationally restricted templates in peptidomimetic design,[18–20] and oxazole-containing inhibitors of antigen presentation by RA-associated HLA-DR proteins have been reported.[21] Herein, we describe the design of three oxazole-modified glycopeptides and explore their effects on class II MHC binding and T-cell recognition. The design was primarily focused on targeting the CIA-associated murine

[a]*Department of Chemistry, Umeå University, SE-901 87 Umeå, Sweden. E-mail: jan.kihlberg@chem.umu.se, anna.linusson@chem.umu.se*
[b]*Medical Inflammation Research, Department of Medical Biochemistry and Biophysics, Karolinska Institute, SE-171 77 Stockholm, Sweden*
[c]*AstraZeneca R&D Mölndal, SE-431 83 Mölndal, Sweden*

† Electronic supplementary information (ESI) available: ^1H NMR and ^{13}C NMR spectra of all new isolated compounds and HPLC chromatograms of the oxazole-modified glycopeptides. See DOI: 10.1039/c003640d

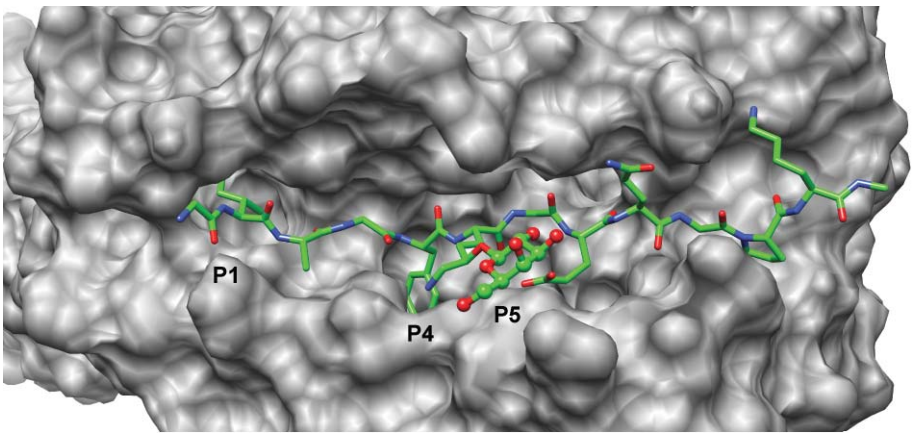

Fig. 1 Comparative model of the class II MHC A^q protein[11] in complex with the CII259-270 glycopeptide from type II collagen. The glycopeptide is bound in an extended conformation with the side chains of Ile^{260} and Phe^{263} anchored in the P1 and P4 pockets of A^q, respectively. The β-D-galactosyl moiety (shown in ball and stick) attached to the side chain of Hyl^{264} in position P5 is extending out of the binding site and is thereby able to interact with a T-cell receptor approaching from above.

A^q system, but the RA-associated human DR4 system was also included in the evaluations. The glycopeptidomimetics are relevant for the DR4 system as well since, as mentioned above, both DR4 and A^q bind and present the CII259-273 epitope.

Results and discussion

Design of oxazole-modified glycopeptides

Oxazole mimetics were designed for the three positions between the important A^q anchoring residues Ile^{260} and Phe^{263} in **1** to prevent cleavage of these peptide bonds, and to investigate binding to A^q as well as T-cell recognition (Fig. 2). The conformationally restricted oxazole scaffold was introduced in the glycopeptide backbone by heterocyclization of the β carbon of one amino acid residue onto the preceding carbonyl group. For the Ala-Gly oxazole **3**, an extra β carbon was added in order to allow the formation of the heterocyclic five-membered ring. In the case of the Gly-Phe oxazole **4**, the oxazole was functionalized with a benzyl instead of a phenyl group, *i.e.* an extra methylene group was added. This introduced more flexibility to facilitate orientation of the aromatic group into the P4 pocket of A^q.

The designed glycopeptidomimetics **2**, **3**, and **4** were docked into the comparative model[11] of A^q to explore the effects of the introduced oxazole moieties on the protein–ligand interactions. Binding poses with anchoring side chains of the oxazole-modified glycopeptides positioned in their respective pockets in the A^q protein were obtained for all designed ligands (Fig. 3). In addition,

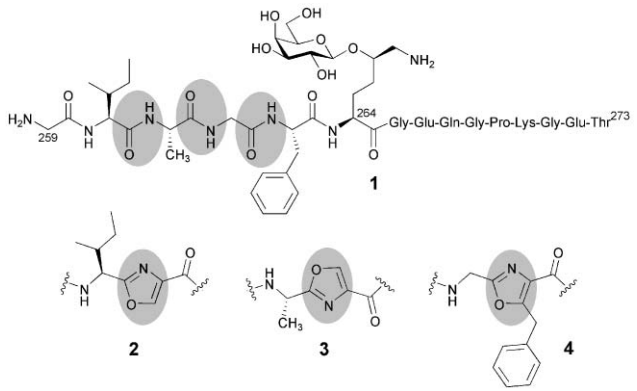

Fig. 2 The CII259-273 glycopeptide (**1**) with the amide bonds between the Ile^{260}-Ala^{261}, Ala^{261}-Gly^{262}, and Gly^{262}-Phe^{263} dipeptide fragments highlighted. Replacement of either of the three indicated amide bonds in **1** with oxazole moieties gave modified CII259-273 glycopeptides with either $Ile^{260}\psi$[oxazole]Ala^{261} (**2**), $Ala^{261}\psi$[oxazole]Gly^{262} (**3**), or $Gly^{262}\psi$[oxazole]Phe^{263} (**4**) bioisosteres.

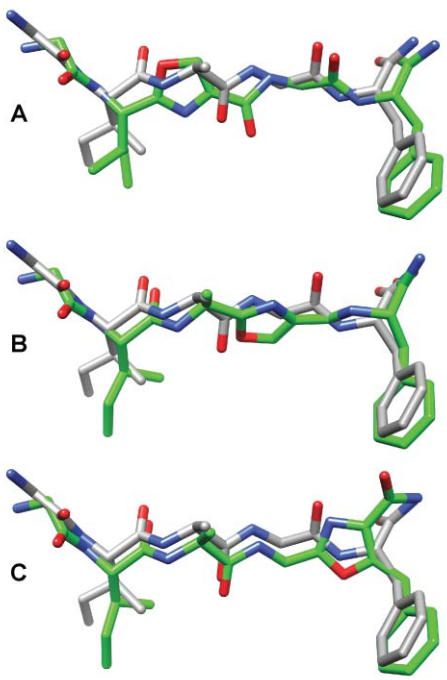

Fig. 3 Docked binding poses for oxazole-modified glycopeptides (carbon atoms colored green) each superposed with the CII259-270 glycopeptide **1** (carbon atoms colored grey), extracted from their respective model of the A^q/glycopeptide complex. Only residues 259 to 263 are shown. The modified glycopeptides are shown in the following order: (A) glycopeptide **2** modified with $Ile^{260}\psi$[oxazole]Ala^{261}, (B) glycopeptide **3** modified with $Ala^{261}\psi$[oxazole]Gly^{262}, and (C) glycopeptide **4** modified with $Gly^{262}\psi$[oxazole]Phe^{263}.

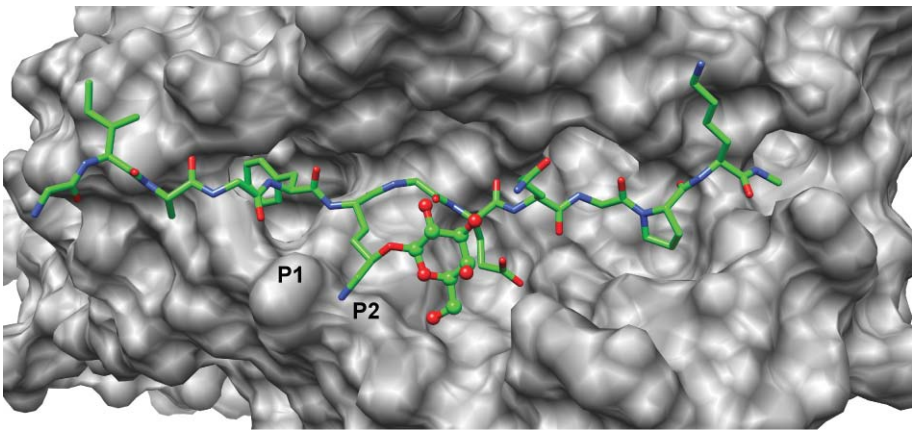

Fig. 4 Proposed model of the complex between DR4 and the CII259-270 glycopeptide from type II collagen based on a DR4 crystal structure.[22] The glycopeptide is primarily anchored by the side chain of residue Phe^{263} in the P1 pocket of DR4. Gly^{262} is positioned in the vicinity of the P1 pocket while Ile^{260} and Ala^{261} are positioned on the binding site border. The β-D-GalHyl^{264} residue (Gal in ball and stick) in position P2 is extending out of the binding site, as in the complex with A^q.

the oxygen and nitrogen atoms in the oxazole rings of the Ile-Ala oxazole **2** and Ala-Gly oxazole **3** were located in the vicinity of the corresponding atoms in the original amide bonds after superposition with the modeled complex of the CII259-273 glycopeptide **1** and A^q. In the case of the Gly-Phe oxazole **4**, docking revealed that there was an oxygen–nitrogen atom mismatch, although this would still allow for hydrogen-donor–acceptor interactions (Fig. 3).

A model of the CII259-270 glycopeptide in complex with a DR4 crystal structure[22] was constructed to explore how the three modified glycopeptides could bind in the DR4 binding site (Fig. 4). As discussed above, the DR4 epitope is shifted three amino acids towards the C terminus of CII259-273 compared to the complex of CII259-273 and A^q. Assuming a similar binding mode as for the CII259-273 glycopeptide **1**, the Ile^{260}-Ala^{261} and Ala^{261}-Gly^{262} oxazole moieties in **2** and **3**, respectively, would be positioned on the border of the DR4 binding site. The Gly^{262}-Phe^{263} oxazole moiety in **4** would, however, be positioned in the vicinity of the P1 pocket in the modeled DR4 complex.

Synthesis of oxazole dipeptide mimetics

Oxazole dipeptide mimetics were synthesized suitably protected for Fmoc-based solid-phase peptide synthesis. The Boc protected Ile-Ala and Ala-Gly oxazole derivatives **5**[23] and **6**[24,25] (Scheme 1) were synthesized as described earlier. From these intermediates, the target molecules **7** and **8** were easily obtained in three steps by hydrolysis of the methyl ester and Boc deprotection, followed by Fmoc protection. The Gly-Phe oxazole derivative was prepared by deprotonation of Schiff base **9** with sodium hydride followed by reaction with phenylacetaldehyde (Scheme 2). After work-up, the crude was immediately subjected to acidic aqueous hydrolysis to give **10**, followed by coupling with Boc-protected glycine to afford **11** (50% yield from **9**). Oxidation with Dess–Martin periodinane to give **12** followed by cyclodehydration using

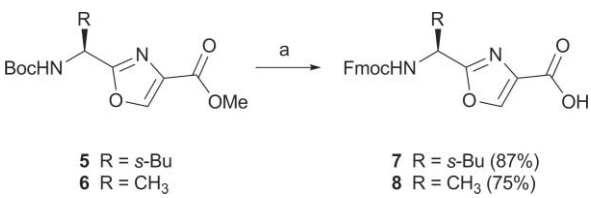

Scheme 1 Synthesis of Ile-Ala and Ala-Gly oxazole derivatives **7** and **8**. *Reagents and conditions*: (a) *i*) LiOH, H_2O, MeOH, rt; *ii*) TFA, CH_2Cl_2, rt; *iii*) FmocOSu, $NaHCO_3$, H_2O, acetone, rt.

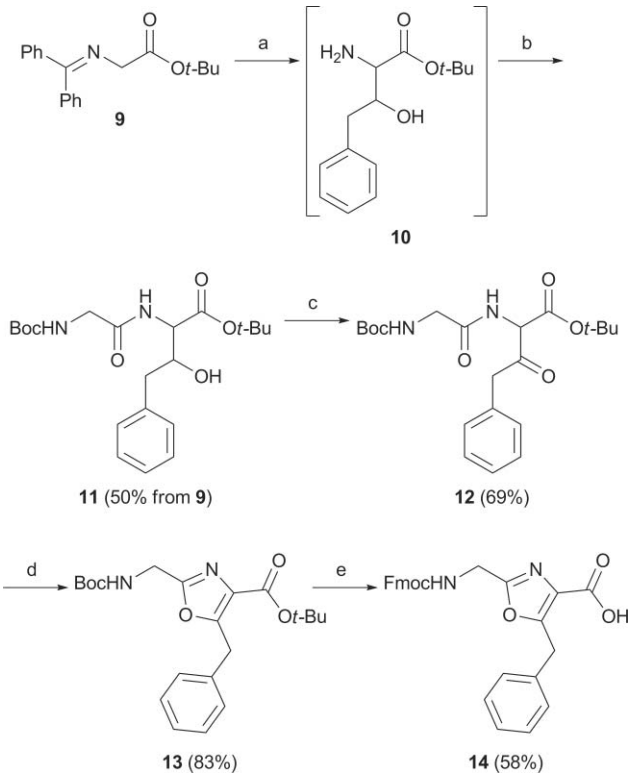

Scheme 2 Synthesis of Gly-Phe oxazole derivative **14**. *Reagents and conditions*: (a) *i*) NaH, phenylacetaldehyde, THF, −78 → 0 °C; *ii*) HCl (1 M aq), THF, 0 °C; (b) Boc-Gly-OH, EDC·HCl, HOAt, Et_3N, CH_2Cl_2, rt; (c) Dess–Martin periodinane, CH_2Cl_2, rt; (d) PPh_3, I_2, Et_3N, CH_2Cl_2, 0 °C → rt; (e) *i*) TFA, CH_2Cl_2, rt; *ii*) FmocOSu, $NaHCO_3$, H_2O, acetone, rt.

triphenylphosphine, iodine, and triethylamine afforded the highly functionalized oxazole intermediate **13**.[26] The Boc and *t*-Bu groups were removed with TFA followed by *N*-Fmoc protection to furnish the target Gly-Phe mimetic **14**. Oxazole dipeptide mimetics **7**, **8**, and **14** were finally incorporated into the CII259-273 glycopeptide using solid-phase peptide synthesis to afford the corresponding oxazole-modified glycopeptides **2**, **3**, and **4** (Fig. 2) in 28–33% yield and >98% purity. The structures of these glycopeptidomimetics were confirmed by ^{1}H NMR spectroscopy and MALDI-TOF mass spectrometry.

Immunological evaluation

The oxazole-modified glycopeptides were evaluated in two different assay systems (Fig. 5 and 6). First, competitive binding experiments were performed to study glycopeptide binding to the murine A^q and human DR4 proteins, respectively. Second, the ability to stimulate A^q and DR4 restricted T-cell hybridomas specific for CII259-273 carrying the GalHyl^{264} moiety were tested using IL-2 secretion as read out.

In the A^q binding assay, only a weak tendency of binding was observed for Ala-Gly oxazole **3** at the highest tested concentration (500 μM) while Ile-Ala oxazole **2** and Gly-Phe oxazole **4** displayed no affinity (Fig. 5). In line with these results, the A^q-restricted T-cell hybridoma HCQ.3 also produced a weak response for **3** at 150 μM, while **2** and **4** did not induce T-cell responses. Hence, the introduced oxazole moieties were not well tolerated in the A^q system. It is noteworthy that both binding to A^q and recognition by T-cell hybridoma HCQ.3 were lost completely when the modified dipeptide moiety involved one of the residues that anchor CII259-273 in A^q, that is Ile^{260} or Phe^{263} (Fig. 1 and 2). The Ala^{261}-Gly^{262} position in between the two anchoring residues was, however, somewhat more tolerant towards the introduced oxazole bioisostere. This position has previously been modified by three different amide bond isosteres, where both the ketomethylene and the (*E*)-alkene isostere were well tolerated in binding to A^q.[11] The ketomethylene isostere also induced strong responses in a panel of T-cell hybridomas, and this further illustrates the tolerance towards modifications of this position in CII259-273.

In the DR4 binding experiment, it was found that all oxazole-modified glycopeptides bound to DR4 (Fig. 6). However, Ile-Ala oxazole **2**, Ala-Gly oxazole **3**, and unmodified glycopeptide **1** displayed significantly higher affinity than Gly-Phe oxazole **4** at the highest test concentration (500 μM). As illustrated in the model of the complex between CII259-270 and DR4 (Fig. 4) the oxazole moieties of **2** and **3** are positioned on the DR4 binding site border. In contrast, the Gly-Phe oxazole moiety in **4** is found in the vicinity of the P1 pocket, where it influences binding negatively. Interestingly, both Ile-Ala oxazole **2** and Ala-Gly oxazole **3** elicited a strong response by the DR4-restricted T-cell hybridoma hDR11.2 while Gly-Phe oxazole **4** was not recognized (Fig. 6). Hybridoma mDR17.2 also recognized **2** strongly, while both **3** and **4** failed to activate this hybridoma. Thus, mDR17.2 seemed to be more sensitive towards oxazole modifications closer to the DR4 binding site than hDR11.2. Overall, recognition of oxazole-modified glycopeptides **2**–**4** by the two T-cell hybridomas agreed well with the DR4 binding data and with the model of the complex between CII259-270 and DR4.

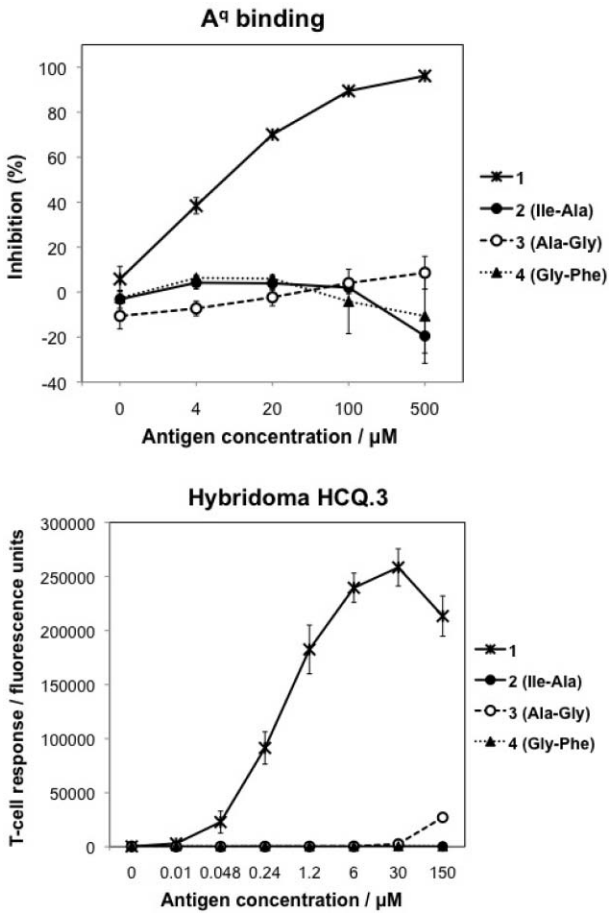

Fig. 5 *Top*: Inhibition of binding of a fixed concentration of biotinylated CII259-273 Lys^{264} peptide to recombinant A^q protein upon incubation with increasing concentrations of glycopeptides **1**, **2**, **3**, or **4**, respectively (the modified position is indicated within parentheses). A^q-bound biotinylated CII259-273 Lys^{264} peptide was detected in a time-resolved fluoroimmunoassay using europium-labeled streptavidin. The points represent the average of triplicates and error bars are set to ± one standard deviation. *Bottom*: Response of the A^q restricted T-cell hybridoma HCQ.3 after incubation with syngeneic spleen cells and increasing concentrations of glycopeptides **1**, **2**, **3**, or **4**, respectively (the modified position is indicated within parentheses). Glycopeptide binding to A^q proteins on the spleen cells allows recognition by HCQ.3, resulting in IL-2 secretion into the supernatant. Secreted IL-2 was subsequently quantified by a sandwich ELISA using the DELFIA system. The points represent the average of triplicates and error bars are set to ± one standard deviation. *Note*: The standard deviation for **3** at 150 μM is too small to be seen visually.

Conclusions

Three oxazole analogues of the CII259-273 glycopeptide have been designed and synthesized. Their ability to bind to the CIA-associated murine A^q and RA-associated human DR4 proteins were evaluated, as well as their ability to induce an immune response in T-cell hybridomas restricted by these class II MHC proteins. The oxazole modifications were not well tolerated in the A^q system where binding to A^q and the T-cell response either was drastically reduced or completely abolished. In the DR4 system, the Ile-Ala and Ala-Gly oxazoles bound well to DR4 and also elicited strong immune responses by one or both of the DR4-restricted T-cell hybridomas. Thus, these two

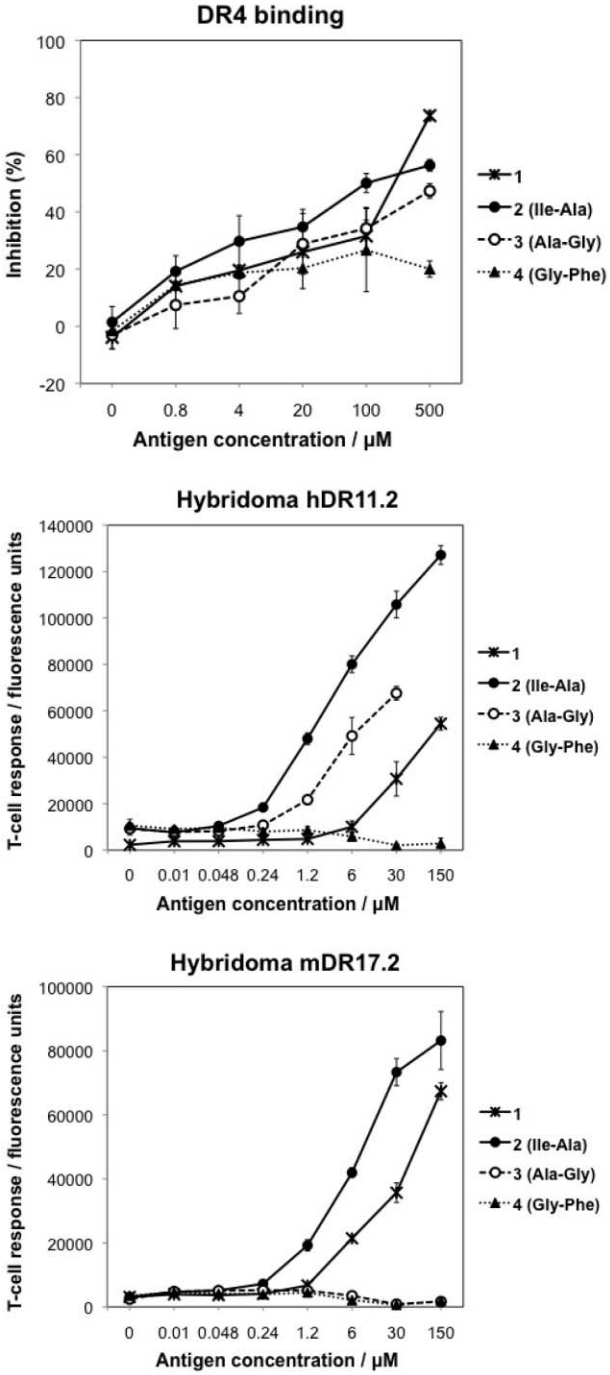

Fig. 6 *Top*: Inhibition of binding of a fixed concentration of biotinylated CLIP peptide to recombinant DR4 protein upon incubation with increasing concentrations of glycopeptides **1**, **2**, **3**, or **4**, respectively (the modified position is indicated within parentheses). The points represent the average of duplicates and error bars are set to ± one standard deviation. *Middle and bottom*: Response of DR4 restricted T-cell hybridomas hDR11.2 and mDR17.2 after incubation with syngeneic spleen cells and increasing concentrations of glycopeptides **1**, **2**, **3**, or **4**, respectively (the modified position is indicated within parentheses). The points represent the average of triplicates and error bars are set to ± one standard deviation. The assays are described further in the legend of Fig. 5 and in detail in the experimental section.

glycopeptidomimetics could be of interest for vaccination studies in mice expressing human DR4 protein and human CD4 co-receptor, in particular if the oxazoles provide stabilization towards enzymatic degradation. Moreover, it can be concluded that neither A^q nor DR4 tolerated the oxazole bioisostere motif when it included an anchoring residue. The results presented in this paper and related studies[11,12] form a basis for selecting altered MHC ligands for *in vivo* evaluation in autoimmune disease models with the long-term goal of developing a therapeutic vaccine for RA.

Experimental section

Molecular modeling

The molecular graphics images were produced using the UCSF Chimera package[27] from the Resource for Biocomputing, Visualization, and Informatics at the University of California, San Francisco (supported by NIH P41 RR-01081).

Modeling of CII259-270 glycopeptide bound to A^q. Backbone coordinates for CII259-270 were directly sampled from the pdb file (pdb code 1MUJ[28]) of a crystal structure of a human CLIP peptide bound to the A^b protein. The peptide sequences were manually aligned so that Ile^{260} of CII259-270 overlapped with Met^{91} of CLIP positioned in the P1 pocket of A^b. One hundred independent models were constructed for the side chains in CII259-270 that differed from the ones in CLIP using a Boltzmann-weighted randomized modeling procedure as implemented in MOE[29] without energy minimization. Selection of side chain conformations of CII259-270 was guided by the indicated rotamer preference of the ligands found in the template[28] and two other related crystal structures (pdb codes 1LNU[30] and 2IAD[31]). These crystal structure proteins had more than 90% sequence identity with A^q in the binding site. The ability of the rotamers to participate in hydrogen bonds, hydrophobic and π-interactions, as well as steric factors with amino acids in the comparative model of the A^q protein[11] were also considered. Hydroxylation and subsequent glycosylation of the Lys^{264} side chain and capping of the C terminal with *N*-methyl amide were done manually. The CII259-270 glycopeptide was energy minimized with the comparative model of the A^q protein in two steps using MacroModel, within Maestro.[32] First, the complex was minimized with the protein backbone atoms constrained with a force constant of 100 kJ mol^{-1} $Å^2$ and the maximum number of iterations set to 1000. Second, minimization was performed without any constraints and the maximum number of iterations set to 5000. All other parameters were at their default settings.

Modeling of CII259-270 glycopeptide bound to DR4. The CII259-270 glycopeptide modeled above (but not energy minimized with A^q) was superposed with the collagen ligand in the DR4 crystal structure[22] (pdb code 2SEB) so that Phe^{263} was positioned in the P1 pocket of DR4 using the MOE[29] software. Energy minimization of the CII259-270/DR4 complex was performed in two steps using MacroModel within Maestro,[32] as described above.

Docking study. The oxazole-modified CII259-267 glycopeptides, with *N*-methyl amide capped C terminals, were docked into the binding site of the A^q comparative model[11] using GOLD.[33–35] The initial 3D conformations of the modified glycopeptides were

generated from smiles using the CORINA[36] software. The binding site was defined as a radius of 18 Å from the x-, y-, and z-coordinates 49.76, 34.94, and 78.55, respectively. A docking constraint was set to prevent orientation of Lys^{264} down in the P4 pocket, as biological results show that the galactose moiety points out of the binding site to make contact with the T-cell receptors.[7,8] More specifically, the Lys^{264} Nε atom of CII259-267 and the βGlu^{14} Cα atom located in the P4 pocket of A^q were restricted to be at least 10 Å apart and at most 20 Å apart. The dockings were terminated after 50 genetic algorithm (GA) runs and default parameter settings were used, except for the following:[37] *popsiz* 140, *n_islands* 4, *maxops* 75000, *niche_siz* 6, *migratewt* 14, *initial_virtual_pt_match_max* 6.0, and *start_vdw_linear_cutoff* 3. The generated docking poses of the modified glycopeptides were energy minimized in the A^q binding site using the Dock function in MOE[29] with the MMFF94x force field and only including A^q residues with atoms within 7 Å of the ligand.

The docked and refined binding poses of the oxazole-modified glycopeptides were compared to the modeled CII259-270 glycopeptide based on shape-based similarity of the sequence Gly^{259}-Phe^{263}-N. The top ranked pose for each ligand was selected based on its ShapeTanimoto value calculated with ROCS.[38]

Chemistry

Compounds **5**[23] and **6**[24,25] were synthesized as described in the cited literature references. All reactions were carried out under an inert atmosphere with dry solvents under anhydrous conditions, unless otherwise stated. CH_2Cl_2 was distilled from calcium hydride whereas THF was distilled from potassium. DMF was distilled under reduced pressure and then dried over 3 Å molecular sieves. MeOH was dried over 3 Å molecular sieves. TLC analysis was performed on silica gel 60 F254 (Merck) with detection by UV light and staining with alkaline aqueous $KMnO_4$ followed by heating. Flash column chromatography was performed on silica gel (Matrex, 60 Å, 35–70 µm, Grace Amicon). Optical rotations were measured with a Perkin-Elmer model 343 polarimeter at 20 °C. ^1H and ^{13}C NMR spectra of the building blocks and their intermediates were recorded at 298 K on a Bruker DRX-400 spectrometer at 400 and 100 MHz, respectively, and calibrated using the residual peak of solvent as internal standard [$CDCl_3$ ($CHCl_3$ δ_H 7.26 ppm, $CDCl_3$ δ_C 77.0 ppm), CD_3OD (CD_2HOD δ_H 3.31 ppm, CD_3OD δ_C 49.0 ppm) and DMF-d_7 (DMF-d_6 δ_H 2.92 and 2.75, DMF-d_7 δ_C 34.89 and 29.76)]. *J* values are given in Hz. First-order chemical shifts and coupling constants were obtained from one-dimensional spectra; carbon and proton resonances were assigned from COSY, NOESY and HETCOR experiments. ^1H NMR spectra of glycopeptides **2**, **3** and **4** were recorded at 298 K on a Bruker Avance spectrometer at 500 MHz in H_2O–D_2O (9 : 1) with H_2O (δ_H 4.76) as internal standard. COSY, TOCSY, ^1H-^{13}C-HSQC and ROESY experiments were used for assignment of proton resonances and determination of chemical shifts. HRMS data were recorded with electrospray ionization (ESI^+). Analytical reversed-phase HPLC was performed on a Beckman System Gold HPLC equipped with a Supelco Discovery® Bio Wide Pore C18 column (250 × 4.6 mm, 5 µm) using a flow-rate of 1.5 mL min^{-1} and detection at 214 nm. Preparative reversed-phase HPLC was performed using a Supelco Discovery® Bio Wide Pore C18 column (250 × 21.2 mm, 5 µm) using the same eluent as for the analytical HPLC, a flow-rate of 11 mL min^{-1}, and detection at 214 nm.

General procedure for hydrolysis of methyl ester, Boc deprotection, and Fmoc protection (7 and 8). LiOH (2 equiv.) dissolved in H_2O (1.8 mL/mmol methyl ester) was added dropwise to methyl ester **5** or **6** (1 equiv.) dissolved in MeOH (5.7 mL/mmol methyl ester) at 0 °C followed by stirring for 40 min. The cooling bath was removed and the solution was stirred for an additional 80–95 min. The methanol was removed under reduced pressure, ethyl acetate and H_2O were added, and the aqueous phase was acidified by addition of HCl (1 M, aq). The phases were separated and the aqueous phase was extracted with ethyl acetate. The combined organic phases were dried over Na_2SO_4, filtered, and concentrated under reduced pressure. The obtained crude carboxylic acids were used without further purification. Trifluoroacetic acid (2 mL/mmol methyl ester) was added to the carboxylic acid (1 equiv.) dissolved in CH_2Cl_2 (9.7 mL/mmol methyl ester) followed by stirring for 1 h at rt. The solution was concentrated and the residue was redissolved in chloroform and concentrated three times to remove residual trifluoroacetic acid. The residue was dissolved in H_2O (5.7 mL/mmol methyl ester) and $NaHCO_3$ (3.4 equiv.) was added, followed by addition of acetone (5.7 mL/mmol methyl ester) and *N*-(9-fluorenylmethoxycarbonyloxy)succinimide (1.05 equiv.). After stirring for 6 h at rt, the acetone was removed under reduced pressure and $CHCl_3$ was added. The aqueous phase was acidified by addition of HCl (1 M, aq) and the phases were separated. The aqueous phase was extracted with $CHCl_3$, and the combined organic phases were then washed with brine, dried over Na_2SO_4, filtered and concentrated under reduced pressure. The residue was purified by flash chromatography (*n*-heptane–EtOAc–AcOH 4 : 1 : 1%→1 : 1 : 1%).

*2-[1-(S)-(9H-Fluoren-9-ylmethoxycarbonylamino)-2-(S)-methyl-butyl]-oxazole-4-carboxylic acid (**7**).* The general procedure described above applied to **5**[23] (270 mg, 0.867 mmol) afforded the Fmoc-protected building block **7** (273 mg, 75%) as a white amorphous solid. $[\alpha]_D^{20}$ −49.0 (*c* 1.0 in MeOH). ^1H NMR (CD_3OD): δ 8.41 (s, 1H, oxazole CH), 7.76 (d, J = 7.5 Hz, 2H, Fmoc-arom), 7.66–7.61 (m, 2H, Fmoc-arom), 7.39–7.33 (m, 2H, Fmoc-arom), 7.30–7.25 (m, 2H, Fmoc-arom), 4.73–4.67 (m, 1H, NCH), 4.45–4.32 (m, 2H, Fmoc-CH_2), 4.18 (t, J = 6.6 Hz, 1H, Fmoc-CH), 2.03–1.91 (m, 1H, C*H*CH_3), 1.59–1.47 (m, 1H, C*H*$_2$$CH_3$), 1.29–1.16 (m, 1H, C*H*$_2$$CH_3$), 0.91 (t, J = 7.4 Hz, 3H, CH_2C*H*$_3$), 0.82 (d, J = 6.8 Hz, 3H, CHC*H*$_3$); ^{13}C NMR (CD_3OD): δ 166.3, 164.1, 158.4, 145.6, 145.2 and 145.1 (1C), 142.6, 134.7, 128.7, 128.1 (splitted), 126.2, 120.9, 67.8 (Fmoc-CH_2), 55.4 (NCH), 48.5 (Fmoc-CH), 39.4 (*C*HCH$_3$), 26.3 (*C*H$_2$CH$_3$), 15.8 (CH*C*H$_3$), 11.2 (CH$_2$*C*H$_3$). HRMS (ESI^+) calcd for $[M + H]^+$ 421.1758, found 421.1745.

*2-[1-(S)-(9H-Fluoren-9-ylmethoxycarbonylamino)-ethyl]-oxazole-4-carboxylic acid (**8**).* The general procedure described above applied to **6**[24,25] (267 mg, 0.988 mmol) afforded the Fmoc-protected building block **8** (325 mg, 87%) as a white amorphous solid. $[\alpha]_D^{20}$ −51.3 (*c* 1.0 in MeOH). ^1H NMR (CD_3OD): δ 8.41 (s, 1H, oxazole CH), 7.77 (d, J = 7.5 Hz, 2H, Fmoc-arom), 7.67–7.61 (m, 2H, Fmoc-arom), 7.40–7.34 (m, 2H, Fmoc-arom), 7.33–7.26 (m, 2H, Fmoc-arom), 4.96–4.89 (m, 1H, NCH), 4.37 (d, J = 6.7 Hz, 2H, Fmoc-C*H*$_2$), 4.20 (t, J = 6.7 Hz, 1H, Fmoc-C*H*),

1.54 (d, J = 7.1 Hz, 3H, CH_3); ^{13}C NMR (CD_3OD): δ 167.4, 163.9, 158.1, 145.9, 145.2, 142.6, 134.6, 128.8, 128.1 (splitted), 126.2 (splitted), 120.9, 67.9 (Fmoc-CH_2), 48.4 (Fmoc-CH), 46.4 (NCH), 19.1 (CH_3). HRMS (ESI$^+$) calcd for $[M + H]^+$ 379.1288, found 379.1274.

2-(*R*/*S*)-(2-*tert*-Butoxycarbonylamino-acetylamino)-3-(*R*/*S*)-hydroxy-4-phenyl-butyric acid *tert*-butyl ester (11). Sodium hydride (60% dispersion in mineral oil, 240 mg, 6.00 mmol) was added in one portion at 0 °C to *N*-(diphenylmethylene)glycine *tert*-butyl ester (1.53 g, 5.17 mmol) dissolved in THF (32 mL). After stirring for 15 min, the solution was cooled to −78 °C, and after an additional 15 min, freshly distilled phenylacetaldehyde (0.90 mL, 8.05 mmol) was added dropwise over 10 min. Stirring was continued at −78 °C for 45 min, and the mixture was then allowed to reach 0 °C and was stirred an additional 2 h. The reaction was quenched by addition of ice-cold $NaHCO_3$ (aq, satd), the phases were separated and the aqueous phase was extracted with EtOAc. The combined organic phases were washed with brine, dried over Na_2SO_4, filtered and concentrated under reduced pressure. The crude product was dissolved in THF (140 mL), and aqueous HCl (1 M, 17.5 mL) was added at 0 °C followed by stirring for 70 min. The THF was removed under reduced pressure, CH_2Cl_2 was added and the aqueous phase was neutralized by addition of $NaHCO_3$ (aq, satd). The phases were separated and the aqueous phase was extracted with CH_2Cl_2. The combined organic phases were dried over Na_2SO_4, filtered, and concentrated. The residue was filtered through a plug of silica (CH_2Cl_2–MeOH 1 : 0→50 : 1) to afford amino alcohol **10** (1.01 g), which was used without further purification in the next step. *N*-(*tert*-Butoxycarbonyl)glycine (703 mg, 4.01 mmol), *N*-ethyl-*N*′-(3-dimethylaminopropyl)carbodiimide hydrochloride (EDC·HCl, 807 mg, 4.21 mmol) and 1-hydroxy-7-azabenzotriazole (HOAt, 573 mg, 4.21 mmol) were added to **10** (1.01 g, 4.0 mmol) dissolved in CH_2Cl_2 (8 mL) at rt. The mixture was stirred for 5 min and then triethylamine (0.36 mL, 4.44 mmol) was added dropwise. After stirring for 12 h, H_2O (5 mL) was added and the phases were separated. The aqueous phase was extracted with CH_2Cl_2 and the combined organic phases were dried over Na_2SO_4, filtered, and concentrated. The residue was purified by flash column chromatography (*n*-heptane–EtOAc 4 : 1→1 : 1) to afford **11** (1 : 1 mixture of diastereomers, 1.07 g, 50% from **9**) as a white foam. ^{1}H NMR ($CDCl_3$) (1 : 1 mixture of diastereomers): δ 7.34–7.19 (m, 10H, Ph), 7.02 (d, J = 6.8 Hz, 1H, NHCH), 6.82 (d, J = 8.4 Hz, 1H, NHCH), 5.24–5.17 (m, 1H, NHCH$_2$), 5.17–5.09 (m, 1H, NHCH$_2$), 4.64–4.59 (m, 2H, NHCH), 4.31 (ddd, J = 9.1, 4.6, and 2.3 Hz, 1H, CHOH), 4.22 (ddd, J = 7.2, 6.5, and 2.9 Hz, 1H, CHOH), 3.93–3.85 (m, 2H, NCH$_2$), 3.85–3.79 (m, 2H, NCH$_2$), 2.85 (dd, J = 13.8 and 4.6 Hz, 1H, CH_2Ph), 2.80 (d, J = 6.5 Hz, 2H, CH_2Ph), 2.71 (dd, J = 13.8 and 9.1 Hz, 1H, CH_2Ph), 1.48 (s, 9H, C(CH$_3$)$_3$), 1.47 (s, 9H, C(CH$_3$)$_3$), 1.46 (s, 9H, C(CH$_3$)$_3$), 1.45 (s, 9H, C(CH$_3$)$_3$); ^{13}C NMR ($CDCl_3$) (1 : 1 mixture of diastereomers): δ 170.3, 169.8, 169.7, 168.7, 156.0 (2C, broad), 137.8 (Ph), 137.3 (Ph), 129.43 (Ph), 129.38 (Ph), 128.7 (Ph), 128.5 (Ph), 126.8 (Ph), 126.6 (Ph), 83.3 (*C*(CH$_3$)$_3$), 82.7 (*C*(CH$_3$)$_3$), 80.5 (*C*(CH$_3$)$_3$), 80.3 (*C*(CH$_3$)$_3$), 74.1 (CH$_2$OH), 73.1 (CH$_2$OH), 58.2 (NHCH), 56.2 (NHCH), 44.3 (2C, NHCH$_2$), 40.4 (*C*H$_2$Ph), 39.6 (*C*H$_2$Ph), 28.3 (C(*C*H$_3$)$_3$), 28.3 (C(*C*H$_3$)$_3$), 28.0 (C(*C*H$_3$)$_3$), 28.0 (C(*C*H$_3$)$_3$).

2-(2-*tert*-Butoxycarbonylamino-acetylamino)-3-oxo-4-phenyl-butyric acid *tert*-butyl ester (12). Alcohol **11** (603 mg, 1.48 mmol) dissolved in CH_2Cl_2 (15 mL) was treated with Dess–Martin periodinane (4.6 mL, 2.22 mmol, 15 wt% solution in CH_2Cl_2) at rt. After stirring for 75 min, $Na_2S_2O_3$ (aq, satd, 5 mL) and $NaHCO_3$ (aq, satd, 5 mL) were added followed by stirring for 20 min. The phases were separated and the aqueous phase was extracted with CH_2Cl_2. The combined organic phases were dried over Na_2SO_4, filtered, and concentrated. Purification with flash chromatography (*n*-heptane–EtOAc 3 : 1) afforded **12** (414 mg, 69%) as a colorless oil. ^{1}H NMR ($CDCl_3$): δ 7.36–7.25 (m, 3H, Ph), 7.22–7.19 (m, 2H, Ph), 7.10 (d, J = 6.1 Hz, 1H, NHCH), 5.24 (d, J = 6.1 Hz, 1H, NCH), 5.10 (br s, 1H, NHCH$_2$), 4.07–3.97 (m, 2H, CH_2Ph), 3.88–3.83 (m, 2H, NCH_2), 1.48 (s, 9H, C(CH$_3$)$_3$), 1.45 (s, 9H, C(CH$_3$)$_3$); ^{13}C NMR ($CDCl_3$): δ 198.8, 169.2 (splitted), 164.5, 155.9 (broad), 132.6 (Ph), 129.6 (Ph), 128.7 (Ph), 127.4 (Ph), 84.4 (*C*(CH$_3$)$_3$), 80.4 (broad, *C*(CH$_3$)$_3$), 62.3 (NCH), 47.6 (*C*H$_2$Ph), 44.0 (NCH$_2$), 28.2 (C(*C*H$_3$)$_3$), 27.9 (C(*C*H$_3$)$_3$).

5-Benzyl-2-(*tert*-butoxycarbonylamino-methyl)-oxazole-4-carboxylic acid *tert*-butyl ester (13). Ketone **12** (396 mg, 0.98 mmol) dissolved in CH_2Cl_2 (15 mL) was treated with PPh_3 (516 mg, 1.97 mmol), I_2 (503 mg, 1.98 mmol), and Et_3N (0.32 mL, 3.95 mmol) at 0 °C. After stirring for 30 min, the cooling bath was removed and the reaction mixture was stirred an additional 2 h. H_2O (10 mL) was then added followed by stirring for 1 h. The phases were separated and the aqueous phase was extracted with CH_2Cl_2. The combined organic phases were dried over Na_2SO_4, filtered, and concentrated. Purification with flash chromatography (*n*-heptane–EtOAc 4 : 1) afforded **13** (315 mg, 83%) as a colorless oil. ^{1}H NMR ($CDCl_3$): δ 7.33–7.21 (m, 5H, Ph), 5.15 (br s, 1H, NH), 4.41–4.34 (m, 2H, NCH$_2$), 4.32 (s, 2H, CH_2Ph), 1.59 (s, 9H, C(CH$_3$)$_3$), 1.43 (s, 9H, C(CH$_3$)$_3$); ^{13}C NMR ($CDCl_3$): δ 161.0, 159.6, 156.7, 155.4, 136.1 128.7, 128.6, 128.5, 126.9, 82.1 (*C*(CH$_3$)$_3$), 80.0 (broad, *C*(CH$_3$)$_3$), 37.8 (NCH$_2$), 32.0 (*C*H$_2$Ph), 28.2 (2C, C(*C*H$_3$)$_3$).

5-Benzyl-2-[(9*H*-fluoren-9-ylmethoxycarbonylamino)-methyl]-oxazole-4-carboxylic acid (14). Trifluoroacetic acid (0.8 mL) was added to **13** (153 mg, 0.396 mmol) dissolved in CH_2Cl_2 (3.8 mL) followed by stirring for 6 h at rt. The solution was concentrated, and the residue was redissolved in $CHCl_3$ and concentrated three times to remove residual trifluoroacetic acid. The residue was dissolved in H_2O (3.5 mL) and $NaHCO_3$ (166 mg, 1.98 mmol) was added, followed by addition of acetone (3.5 mL) and *N*-(9-fluorenylmethoxycarbonyloxy)succinimide (142 mg, 0.421 mmol). After stirring for 16 h at rt, the acetone was removed under reduced pressure and $CHCl_3$ was added. The aqueous phase was acidified to pH 2 by addition of HCl (1 M, aq) and the phases were separated. The aqueous phase was extracted with $CHCl_3$ and the combined organic phases were then washed with brine, filtered, and concentrated under reduced pressure. Purification by flash chromatography (*n*-heptane–EtOAc–AcOH 4 : 1 : 1%→1 : 2 : 1%) afforded **14** (104 mg, 57%) as a white amorphous solid. ^{1}H NMR (DMF-d_7): δ 8.11 (t, J = 5.6 Hz, 1H, NH), 7.94 (d, J = 7.5 Hz, 2H, Fmoc-arom), 7.76 (d, J = 7.4 Hz, 2H, Fmoc-arom), 7.48–7.41 (m, 2H, Fmoc-arom), 7.38–7.28 (m, 6H, Fmoc-arom and Ph), 7.28–7.21 (m, 1H, Ph), 4.49–4.43 (m, 4H, NCH$_2$ and CH_2Ph), 4.36–4.24 (m, 3H, Fmoc-CH and Fmoc-CH_2); ^{13}C-NMR (DMF-d_7): δ 163.5, 162.6, 160.5, 157.6, 156.9, 144.5, 141.4, 137.3, 129.0,

Table 1 ^{1}H NMR chemical shifts for CII259-273 with Ile^{260}ψ[oxazole]Ala^{261} (**2**)[a]

Residue	NH	Hα	Hβ	Hγ	Others
Gly^{259}		3.87[b]			
Ile^{260}ψ[oxazole]Ala^{261}	8.96	5.02	2.06	1.45, 1.22, 0.87 (CH_3)	0.85 (Hδ), 8.35 (oxazole)
Gly^{262}	8.56	4.02[b]			
Phe^{263}	8.12	4.63	3.09, 3.01		7.21 (Hδ), 7.26 (Hε and Hζ)
Hyl^{264}	8.46	4.26	1.99, 1.75	1.59[b]	4.01 (Hδ), 3.15 and 2.96 (Hε), 7.61 (εNH$_2$), [c]
Gly^{265}	8.02	3.88[b]			
Glu^{266}	8.16	4.34	2.07, 1.91	2.40[b]	
Gln^{267}	8.45	4.36	2.10, 1.96	2.34[b]	7.48 and 6.81 (δNH$_2$)
Gly^{268}	8.25	4.10, 3.97			
Pro^{269}		4.39	2.24, 1.89	1.97[b]	3.56[b] (Hδ)
Lys^{270}	8.44	4.28	1.82, 1.75	1.43[b]	1.66[b] (Hδ), 2.97[b] (Hε), 7.49 (εNH$_2$)
Gly^{271}	8.34	3.93[b]			
Glu^{272}	8.20	4.45	2.14, 1.96	2.45[b]	
Thr^{273}	8.07	4.31	4.31	1.16	

[a] Measured at 500 MHz and 298 K in water containing 10% D_2O with H_2O (δ_H 4.76 ppm) as internal standard. [b] Degeneracy has been assumed. [c] Chemical shifts for the galactose moiety: δ 4.42 (H1), 3.90 (H4), 3.74 (H6), 3.67 (H5), 3.57 (H3), and 3.51 (H2).

128.8, 128.0, 127.4, 127.1, 125.7, 120.4, 66.8 (Fmoc-CH_2), 47.3 (Fmoc-CH), 38.3 (NCH_2), 31.7 (CH_2Ph). HRMS (ESI$^+$) calcd for $[M + H]^+$ 455.1601, found 455.1588.

General procedure for solid-phase glycopeptide synthesis. Glycopeptides **2**, **3**, and **4** were synthesized in mechanically agitated reactors on Tentagel-S-PHB-Thr(*t*Bu)-Fmoc resins using standard solid-phase methodology essentially as described elsewhere.[39] Couplings were performed in DMF and monitored using bromophenol blue as indicator. N^{α}-Fmoc amino acids with standard side-chain protecting groups (4 equiv.) were activated with 1-hydroxybenzotriazole (HOBt, 6 equiv.) and 1,3-diisopropylcarbodiimide (DIC, 3.9 equiv.). (5*R*)-N^{α}-(Fluoren-9-ylmethoxycarbonyl)-N^{ε}-benzyloxycarbonyl-5-*O*-(2,3,4,6-*tetra*-*O*-acetyl-β-D-galactopyranosyl)-5-hydroxy-L-lysine[11,40] (1.5 equiv.) and building blocks **7**, **8** and **14** (1.5 equiv) were activated with *O*-(7-azabenzotriazol-1-yl)-1,1,3,3-tetramethyluronium hexafluorophosphate (HATU, 1.5 equiv) and 2,4,6-collidine (3.0 equiv.) and coupled for 24 h. Fmoc deprotection after each coupling cycle was accomplished by treatment with 20% piperidine in DMF for 10 min. The glycopeptides were cleaved from the resins with trifluoroacetic acid–H_2O–thioanisole–ethanedithiol (35 : 2 : 2 : 1) for 3 h at 40 °C with workup performed essentially as described elsewhere.[39] Purification by reversed-phase HPLC was followed by deacetylation with NaOMe in MeOH (20 mM, 1 mL/mg peptide) for 2–3 h at rt (monitored by analytical reversed-phase HPLC). Neutralization by addition of AcOH and concentration under reduced pressure gave a residue that was purified using reversed-phase HPLC followed by lyophilization.

Glycyl-L-isoleucylψ[oxazole]alanyl-glycyl-L-phenylalanyl-5-O-(β-D-galactopyranosyl)-5-hydroxy-L-lysylglycyl-L-glutam-1-yl-L-glutaminylglycyl-L-prolyl-L-lysylglycyl-L-glutam-1-yl-L-threonine (***2***). Synthesis was performed with building block **7** on solid phase (50 μmol) according to the general procedure described above. This afforded the trifluoroacetate salt of **2** (29.5 mg, 29% yield based on the amount of resin used) as a white amorphous solid after lyophilization. MS (MALDI-TOF) calcd 1649.77 $[M + H]^+$, found 1650.03. ^{1}H NMR data are given in Table 1.

Glycyl-L-isoleucyl-L-alanylψ[oxazole]glycyl-L-phenylalanyl-5-O-(β-D-galactopyranosyl)-5-hydroxy-L-lysylglycyl-L-glutam-1-yl-L-glutaminylglycyl-L-prolyl-L-lysylglycyl-L-glutam-1-yl-L-threonine (***3***). Synthesis was performed with building block **8** on solid phase (51 μmol) according to the general procedure described above. This afforded the trifluoroacetate salt of **3** (34.1 mg, 33% yield based on the amount of resin used) as a white amorphous solid. MS (MALDI-TOF) calcd 1663.81 $[M + H]^+$, found 1663.78. ^{1}H NMR data are given in Table 2.

Glycyl-L-isoleucyl-L-alanyl-glycylψ[oxazole]-L-phenylalanyl-5-O-(β-D-galactopyranosyl)-5-hydroxy-L-lysylglycyl-L-glutam-1-yl-L-glutaminylglycyl-L-prolyl-L-lysylglycyl-L-glutam-1-yl-L-threonine (***4***). Synthesis was performed with building block **14** on solid phase (50 μmol) according to the general procedure described above. This afforded the trifluoroacetate salt of **4** (28.4 mg, 28% yield based on the amount of resin used) as a white amorphous solid after lyophilization. MS (MALDI-TOF) calcd 1663.78 for $[M + H]^+$, found 1663.80. ^{1}H NMR data are given in Table 3.

MHC-peptide binding assay

The inhibition assay was performed in 96-well microtiter assay plates essentially as described elsewhere.[15,41] Briefly, purified soluble recombinant class II MHC proteins (*A^q assay*: 0.5 μM A^q; *DR4 assay*: 1 μM DR4) were incubated with a fixed concentration of a biotinylated tracer peptide (3 μM, *A^q assay*: CII259-273-bio Lys^{264}; *DR4 assay*: CLIP-bio with sequence KPVSKMRMATPLLMQALPM) and increasing concentrations of test peptides **1**, **2**, **3**, or **4** (*A^q assay*: 0, 4, 20, 100, 500 and 2500 μM; *DR4 assay*: 0, 0.8, 4, 20, 100 and 500 μM) in PBS for 48 h at room temperature. This mixture also contained a cocktail of protease inhibitors (Complete™, Boehringer, Mannheim). During this incubation, new 96-well microtiter assay plates were precoated with mAb (10 μg mL^{-1}, *A^q assay*: Y3P 10 mAb; *DR4 assay*: L243 mAb) by incubating for 2 h at room temperature or overnight at 4 °C followed by blocking with PBS containing 2% low fat milk and washing with PBS containing 0.1% Tween 20. 100 μL of the incubated mixtures containing class II MHC proteins, biotinylated

Table 2 ^{1}H NMR chemical shifts for CII259-273 with Ala^{261}ψ[oxazole]Gly^{262} (**3**)[a]

Residue	NH	Hα	Hβ	Hγ	Others
Gly^{259}		3.83[b]			
Ile^{260}	8.46	4.18	1.79	1.40, 1.13, 0.83 (CH_3)	0.81 (Hδ)
Ala^{261}ψ[oxazole]Gly^{262}	8.89	5.13	1.57		8.28 (oxazole),
Phe^{263}	8.30	4.73	3.16		7.27 (Hδ), 7.31 (Hε and Hζ)
Hyl^{264}	8.51	4.31	2.00, 1.74	1.62[b]	4.02 (Hδ), 3.16 and 2.96 (Hε), 7.60 (εNH$_2$), [c]
Gly^{265}	7.98	3.89[b]			
Glu^{266}	8.25	4.36	2.09, 1.94	2.42[b]	
Gln^{267}	8.47	4.36	2.10, 1.96	2.34[b]	7.48 and 6.81 (δNH$_2$)
Gly^{268}	8.26	4.10, 3.97			
Pro^{269}		4.39	2.25, 1.90	1.98[b]	3.57[b] (Hδ)
Lys^{270}	8.44	4.28	1.82, 1.75	1.43[b]	1.66[b] (Hδ), 2.97[b] (Hε), 7.49 (εNH$_2$)
Gly^{271}	8.34	3.94[b]			
Glu^{272}	8.20	4.45	2.14, 1.96	2.45[b]	
Thr^{273}	8.06	4.30	4.30	1.15	

[a] Measured at 500 MHz and 298 K in water containing 10% D_2O with H_2O (δ_H 4.76 ppm) as internal standard. [b] Degeneracy has been assumed. [c] Chemical shifts for the galactose moiety: δ 4.41 (H1), 3.89 (H4), 3.74 (H6), 3.66 (H5), 3.60 (H3), and 3.51 (H2).

Table 3 ^{1}H NMR chemical shifts for CII259-273 with Gly^{262}ψ[oxazole]Phe^{263} (**4**)[a]

Residue	NH	Hα	Hβ	Hγ	Others
Gly^{259}		3.83[b]			
Ile^{260}	8.41	4.16	1.77	1.39, 1.11, 0.82 (CH_3)	0.80 (Hδ)
Ala^{261}	8.42	4.30	1.28		
Gly^{262}ψ[oxazole]Phe^{263}	8.56	4.45			4.76[b] (oxazole-CH_2), 7.24 (Hδ), 7.34 (Hε), 7.28 (Hζ)
Hyl^{264}	8.38	4.45	2.12, 1.92	1.72[b]	4.05 (Hδ), 3.19 and 2.99 (Hε), 7.62 (εNH$_2$), [c]
Gly^{265}	8.73	3.95[b]			
Glu^{266}	8.15	4.36	2.05, 1.87	2.31[b]	
Gln^{267}	8.41	4.34	2.09, 1.94	2.32[b]	7.46 and 6.79 (δNH$_2$)
Gly^{268}	8.20	4.03, 3.91			
Pro^{269}		4.38	2.24, 1.89	1.96[b]	3.53[b] (Hδ)
Lys^{270}	8.43	4.27	1.82, 1.74	1.42[b]	1.65[b] (Hδ), 2.96[b] (Hε), 7.49 (εNH$_2$)
Gly^{271}	8.34	3.93[b]			
Glu^{272}	8.19	4.45	2.14, 1.96	2.45[b]	
Thr^{273}	8.07	4.31	4.31	1.15	

[a] Measured at 500 MHz and 298 K in water containing 10% D_2O with H_2O (δ_H 4.76 ppm) as internal standard. [b] Degeneracy has been assumed. [c] Chemical shifts for the galactose moiety: δ 4.43 (H1), 3.88 (H4), 3.74 (H6), 3.65 (H5), 3.60 (H3), and 3.52 (H2).

tracer peptide, and test peptides in PBS were then transferred to the plates precoated with mAb followed by incubation for 2 h at room temperature or overnight at 4 °C. After washing with PBS, containing 0.1% Tween 20, the amount of biotinylated tracer peptide bound to the recombinant A^{q} or DR4 proteins captured in the wells was quantified using the dissociation-enhanced lanthanide fluoroimmunoassay (DELFIA®) system based on the time-resolved fluoroimmunoassay technique with europium-labeled streptavidin (Wallac, Turku), according to the manufacturers instructions. The A^{q} experiment was performed in triplicates while the DR4 experiment was performed in duplicates.

T-cell activation assay

The response of the glycopeptide-specific and A^{q} or DR4 restricted T-cell hybridoma lines, that is, the amount of IL-2 secreted following incubation of the hybridoma with antigen-presenting spleen cells expressing A^{q} or DR4 and increasing concentrations of the glycopeptides, was determined essentially as described by Michaëlsson *et al.*[42] with slight modifications. In brief, 5×10^4 T-cell hybridomas were co-cultured with 5×10^5 syngeneic spleen cells and increasing concentrations of test peptides **1**, **2**, **3**, or **4** (0, 0.01, 0.048, 0.24, 1.2, 6.0, 30, and 150 μM) in a volume of 200 μL in 96-well flat-bottom microtiter plates. After 24 h, 100 μL aliquots of the supernatants were removed and frozen in order to kill any transferred T-cell hybridomas. The contents of IL-2 in the culture supernatant were measured by sandwich ELISA (purified rat anti-mouse IL-2 as capturing mAb and the biotin rat anti-mouse IL-2 as detecting mAb, both from PharMingen, Los Angeles, CA) using the DELFIA® system (Wallac, Turku, Finland), according to the manufacturers instructions. Recombinant mouse IL-2 served as a positive control. The experiment was performed in triplicates.

Acknowledgements

This work was funded by grants from the Swedish Research Council, the Swedish strategic science foundation (SSF), the

Biotechnology Fund at Umeå University, the JC Kempe Foundation (SJCKMS), and the EU project Masterswitch HEALTH-F2-2008-223404.

References

1 J. S. Courtenay, M. J. Dallman, A. D. Dayan, A. Martin and B. Mosedale, *Nature*, 1980, **283**, 666–668.
2 G. P. Astorga and R. C. Williams Jr, *Arthritis Rheum.*, 1969, **12**, 547–554.
3 P. Stastny, *J. Clin. Invest.*, 1976, **57**, 1148–1157.
4 P. K. Gregersen, J. Silver and R. J. Winchester, *Arthritis Rheum.*, 1987, **30**, 1205–1213.
5 P. H. Wooley, H. S. Luthra, J. M. Stuart and C. S. David, *J. Exp. Med.*, 1981, **154**, 688–700.
6 U. Brunsberg, K. Gustafsson, L. Jansson, E. Michaëlsson, L. Ährlund-Richter, S. Pettersson, R. Mattsson and R. Holmdahl, *Eur. J. Immunol.*, 1994, **24**, 1698–1702.
7 J. Broddefalk, J. Bäcklund, F. Almqvist, M. Johansson, R. Holmdahl and J. Kihlberg, *J. Am. Chem. Soc.*, 1998, **120**, 7676–7683.
8 B. Holm, J. Bäcklund, M. A. F. Recio, R. Holmdahl and J. Kihlberg, *ChemBioChem*, 2002, **3**, 1209–1222.
9 J. Bäcklund, A. Treschow, R. Bockermann, B. Holm, L. Holm, S. Issazadeh-Navikas, J. Kihlberg and R. Holmdahl, *Eur. J. Immunol.*, 2002, **32**, 3776–3784.
10 B. Dzhambazov, K. S. Nandakumar, J. Kihlberg, L. Fugger, R. Holmdahl and M. Vestberg, *J. Immunol.*, 2006, **176**, 1525–1533.
11 I. E. Andersson, B. Dzhambazov, R. Holmdahl, A. Linusson and J. Kihlberg, *J. Med. Chem.*, 2007, **50**, 5627–5643.
12 I. E. Andersson, T. Batsalova, B. Dzhambazov, R. Holmdahl, A. Linusson and J. Kihlberg, unpublished work.
13 E. F. Rosloniec, K. B. Whittington, D. D. Brand, L. K. Myers and J. M. Stuart, *Cell. Immunol.*, 1996, **172**, 21–28.
14 A. Corthay, J. Bäcklund, J. Broddefalk, E. Michaëlsson, T. J. Goldschmidt, J. Kihlberg and R. Holmdahl, *Eur. J. Immunol.*, 1998, **28**, 2580–2590.
15 P. Kjellén, U. Brunsberg, J. Broddefalk, B. Hansen, M. Vestberg, I. Ivarsson, Å. Engström, A. Svejgaard, J. Kihlberg, L. Fugger and R. Holmdahl, *Eur. J. Immunol.*, 1998, **28**, 755–767.
16 J. Bäcklund, S. Carlsen, T. Höger, B. Holm, L. Fugger, J. Kihlberg, H. Burkhardt and R. Holmdahl, *Proc. Natl. Acad. Sci. U. S. A.*, 2002, **99**, 9960–9965.
17 E. C. Andersson, B. E. Hansen, H. Jacobsen, L. S. Madsen, C. B. Andersen, J. Engberg, J. B. Rothbard, G. Sønderstrup McDevitt, V. Malmström, R. Holmdahl, A. Svejgaard and L. Fugger, *Proc. Natl. Acad. Sci. U. S. A.*, 1998, **95**, 7574–7579.
18 M. Falorni, G. Giacomelli, A. Porcheddu and G. Dettori, *Eur. J. Org. Chem.*, 2000, 3217–3222.
19 A. Plant, F. Stieber, J. Scherkenbeck, P. Lösel and H. Dyker, *Org. Lett.*, 2001, **3**, 3427–3430.
20 E. Mann and H. Kessler, *Org. Lett.*, 2003, **5**, 4567–4570.
21 E. F. Rosloniec, T. Brandstetter, S. Leyer, F. W. Schwaiger and Z. A. Nagy, *J. Autoimmun.*, 2006, **27**, 182–195.
22 A. Dessen, C. M. Lawrence, S. Cupo, D. M. Zaller and D. C. Wiley, *Immunity*, 1997, **7**, 473–481.
23 B. Wagner, D. Schumann, U. Linne, U. Koert and M. A. Marahiel, *J. Am. Chem. Soc.*, 2006, **128**, 10513–10520.
24 A. J. Phillips, Y. Uto, P. Wipf, M. J. Reno and D. R. Williams, *Org. Lett.*, 2000, **2**, 1165–1168.
25 A. D. Wist, L. Gu, S. J. Riedl, Y. Shi and G. L. McLendon, *Bioorg. Med. Chem.*, 2007, **15**, 2935–2943.
26 P. Wipf and C. P. Miller, *J. Org. Chem.*, 1993, **58**, 3604–3606.
27 E. F. Pettersen, T. D. Goddard, C. C. Huang, G. S. Couch, D. M. Greenblatt, E. C. Meng and T. E. Ferrin, *J. Comput. Chem.*, 2004, **25**, 1605–1612.
28 Y. Zhu, A. Y. Rudensky, A. L. Corper, L. Teyton and I. A. Wilson, *J. Mol. Biol.*, 2003, **326**, 1157–1174.
29 *MOE (Molecular Operating Environment)*, version 2007.09, Chemical Computing Group Inc., Montreal, Canada.
30 X. Liu, S. Dai, F. Crawford, R. Frugé, P. Marrack and J. Kappler, *Proc. Natl. Acad. Sci. U. S. A.*, 2002, **99**, 8820–8825.
31 C. A. Scott, P. A. Peterson, L. Teyton and I. A. Wilson, *Immunity*, 1998, **8**, 319–329.
32 *Maestro*, version 9.1, Schrödinger, LLC, New York, NY.
33 G. Jones, P. Willett and R. C. Glen, *J. Mol. Biol.*, 1995, **245**, 43–53.
34 G. Jones, P. Willett, R. C. Glen, A. R. Leach and R. Taylor, *J. Mol. Biol.*, 1997, **267**, 727–748.
35 *GOLD (Genetic Optimisation for Ligand Docking)*, version 3.1.1, The Cambridge Crystallographic Datacenter, Cambridge, U. K.
36 *CORINA (COoRdINAtes)*, Molecular Networks GmbH, Nägelsbachstraße 25, 91052 Erlangen, Germany, Accessed Nov 13, 2009.
37 C. D. Andersson, I. E. Andersson, J. Kihlberg and A. Linusson, unpublished work.
38 *ROCS (Rapid Overlay of Chemical Structures)*, version 2.4.2, OpenEye Scientific Software, Inc.: Santa Fe, NM.
39 J. Broddefalk, M. Forsgren, I. Sethson and J. Kihlberg, *J. Org. Chem.*, 1999, **64**, 8948–8953.
40 B. M. Syed, T. Gustafsson and J. Kihlberg, *Tetrahedron*, 2004, **60**, 5571–5575.
41 C. M. Hill, A. Liu, K. W. Marshall, J. Mayer, B. Jorgensen, B. Yuan, R. M. Cubbon, E. A. Nichols, L. S. Wicker and J. B. Rothbard, *J. Immunol.*, 1994, **152**, 2890–2898.
42 E. Michaëlsson, M. Andersson, R. Holmdahl and Å. Engström, *Eur. J. Immunol.*, 1992, **22**, 1819–1825.

